Validation of an Instrumented Hammer for Rhinoplasty Osteotomies: A Cadaveric Study

Justine Giunta, Léo Lamassoure, Lara Nokovitch, Giuseppe Rosi, Anne-Sophie Poudrel, J-P Meningaud, Guillaume Haïat, Romain Bosc

Validation of an Instrumented Hammer for Rhinoplasty Osteotomies: A Cadaveric Study

Short running head: Instrumented Hammer for Rhinoplasty

Justine Giunta, MD[1,2] ; Léo Lamassoure[2] ; Lara Nokovitch, MD[3] ; Giuseppe Rosi[2] ; Anne-Sophie Poudrel[2] ; J-P.Meningaud, MD, PhD[1] ; Guillaume Haïat, PhD[2] ; Romain Bosc, MD, PhD[1,4].

1. Hôpital Henri Mondor, Plastic, Reconstructive, Aesthetic and Maxillofacial Surgery Department, 51 avenue du Maréchal de Lattre de Tassigny, 94000 Créteil, France
2. CNRS, Laboratoire de Modélisation et de Simulation Multi Échelle, UMR CRNS 8208, 61 avenue du Général de Gaulle, Créteil 94010, France
3. Hôpital Beaujon, Maxillo-facial Surgery Department, 100 boulevard du Général Leclerc, 92110 Clichy, France
4. INSERM U955 IMRB, Team 10, 94000 Creteil, France; UPEC Paris Est-Creteil University, Faculty of Medicine, F-94000 Creteil, France

Corresponding author:

Romain Bosc, MD, PhD

Hôpital Henri Mondor, Plastic, Reconstructive, Aesthetic and Maxillofacial Surgery Department, 50 avenue du Maréchal de Lattre de Tassigny, 94000 Créteil, France

Email: romainbosc@gmail.com

Keywords: Rhinoplasty; nasal osteotomy; assisted surgery.

Products & Devices:

- Surgical mallet (32-6906-26, Zepf, Tuttlingen, Germany)
- Piezoelectric sensor (208C04, PCB Piezotronics, Depew, NY, USA)
- Osteotome (32-6002-10, Zepf, Tuttlingen, Germany)
- Data acquisition module (NI 9234, National Instruments, Austin, TX, USA)
- LabVIEW (National Instruments, Austin, TX, USA)
- Matlab (The MathWorks, Inc., Natick, Massachusetts, USA)
- Video camera (L-920M3, Spedal, Taiwan)

Key points:

Question: Is it possible to determine the bone properties around the osteotome tip and the occurrence of fractures with a smart hammer during the nasal osteotomies for rhinoplasties?

Findings: A predictive algorithm was developed to detect the occurrence of fractures, and the close proximity of the osteotome to the frontal bone.

Meaning: Rhinoplasty surgeons may value the ability to have instant feedback while performing nasal osteotomies.

Abstract:

Background: Osteotomies during rhinoplasty are usually based on surgeon's proprioception to determine the number, energy and trajectory of impacts.

Objective: The first objective was to detect the occurrence of fractures. The second objective was to determine when the thicker frontal bone was encountered by the osteotome.

Materials and Methods: An instrumented hammer was used to measure the impact force during lateral osteotomies on 9 human anatomic specimens. A prediction algorithm was developed using machine learning techniques, to detect the occurrence of fractures, and the proximity of the osteotome to the frontal bone.

Results: The algorithm was able to predict the occurrence of fractures and the proximity to the frontal bone with a prediction rate of 83%, 91%, and 93% when allowing for an error of 0, 1, and 2 impacts, respectively. The location of the osteotome in the frontal bone was predicted with an error of 7,7%.

Conclusion: An osteotomy hammer measuring the impact force when performing lateral osteotomies can predict the occurrence of fractures and the proximity to the frontal bone, providing the surgeon with instant feedback.

Introduction:

Rhinoplasty is a common intervention in plastic surgery, representing around 9% of all plastic surgery procedures[1]. It is a complex intervention with a long learning process[2] and risks of complications[3-4], even for an experienced surgeon.

Osteotomies are particularly crucial when taking care of deviated, hunchbacked noses, with a nasal bridge and / or a wide base[5-6], and must be performed with caution to avoid any cosmetic or functional complications that could result in permanent deformities[6-7].

Nasal osteotomies are often performed without direct visual control, guided only by the surgeon's proprioception (touch, hearing). However, it remains difficult to quantify bone density and to define precisely the osteotomy pathway, which would be of interest, especially for lateral osteotomies which are the most prone to variations and complications[8].

Our team developed a prototype of surgical navigational aid, using a hammer instrumented with a piezoelectric force sensor originally designed to determine the stability of hip prosthesis[9-11]. This approach was validated *in vitro*[12], *ex vivo*[13-14] and in Human anatomic specimen[15]. More recently, it was adapted to nasal osteotomies, first *in vitro* with composite materials and bone mimicking phantoms[16], then *ex vivo* in rabbit head samples[17].

Measuring the force generated when performing rhinoplasty osteotomies with this osteotomy hammer might help surgeons to adapt their impact strength, determine the progress of the osteotome through the bone, anticipate an uncontrolled fracture, and obtain objective and quantified information regarding the osteotome pathway. The clinical implementation of this approach could provide the surgeon with objective data regarding the nature of the bone located at the osteotome tip, the presence of a fracture and the proximity of the osteotome to frontal bone, without modifying the operating time, the information being given in real time. It could also help young surgeons to achieve a faster learning curve for rhinoplasty[18].

The objective of the present study was to determine if the piezoelectric device could detect unintended early nasal bone fractures, and the transition from the thinner nasal bone to the thicker nasofrontal junction and frontal bone.

Materials & Methods:

Nine human anatomical specimen with a mean age of 85 ±14 years old were used for the assessment of our instrumented hammer. None had nasal trauma, nasal malformation or nasal surgery.

The study design was approved, and the human anatomical specimen were requested to the Fer à Moulin surgical school of Paris. All donors had previously completed a hand-written, dated and signed statement confirming their wish to donate their body[19].

All osteotomies were performed by the same operator for a matter of reproducibility. An open rhinoplasty technique was performed in order to visualize the motion of the osteotome (video 1). For each subject, two lateral ascending curved osteotomies ("low to high" type[18]) were performed, leading to a total number of 18 osteotomies. The path of the osteotome from its starting point to the frontal bone was always the same, and followed a line drawn beforehand on the nasal pyramid (video 1).

The device used in this study was similar to the one described by Hubert et al.[16] and Lamassoure et al.[17], and allowed to analyze the osteotome force-feedback signal sensed by a piezoelectric sensor placed on a surgical mallet (Fig. 1). A data acquisition module was used to record the signal $s(t)$ corresponding to the variation of the force-feedback signal according to time. The same signal processing method as the one developed *in vitro* was applied, and two indicators τ and λ, respectively related to the rigidity and viscoelasticity of the impacted material, were calculated for each signal[16].

The movements of the osteotome were recorded using a video camera in order to track fracture initiation. After each impact, the state of the bone-osteotome system (BOS) was classified based on the image obtained with the camera and the surgeon proprioception. The BOS was classified into three classes defined as follows: “Fracture” (osteotome tip located in a visible fracture), “Bone” (osteotome tip in bone tissue, no visible fracture), and “Hard Bone” or “HB” (osteotome tip in frontal bone). Based on the aforementioned classification, the impacts were classified into four groups illustrated in Fig. 2, depending on the state of the BOS before and after the impact.

A dedicated iterative algorithm based on machine learning and using Support Vector Machine (SVM) classifications was developed in order to predict the state of the BOS after each impact I_n. The algorithm was applied to all 531 impacts corresponding to 18 osteotomies.

Classification #A was applied for all impacts and aimed at determining whether the BOS after the impact belonged to the “Hard Bone” state or to other states. Classification #B was applied when the state of the BOS before the impact I_n belonged to the “Bone” state and aimed at determining whether the BOS after the impact *In* belonged to the “Bone” or “Fracture” state. Classification #C was applied when the state of the BOS before the impact I_n belonged to the “Fracture” state and aimed at determining whether the BOS after the impact I_n belonged to the “Bone” or “Fracture” state.

The BOS state of the first impact was initialized as “Bone”. Then, for each impact I_n (n>1 corresponding to the impact number), the algorithm used four input parameters to determine to state of the BOS of I_n:

- the state of the BOS for the impact I_{n-1} (“Bone”, “Fracture”, “HB”)
- the value of $\tau_n=\tau$ corresponding to the impact I_n
- the value of $\Delta\tau_n = \tau_n - \tau_{n-1}$, where τ_{n-1} corresponds to the value of τ for the impact I_{n-1}
- the value of $\lambda_n = \lambda$ corresponding to the impact I_n

Finally, the state of the BOS predicted by the algorithm was compared to the state of the BOS observed with the video tracking analysis.

Descriptive statistics were produced using Excel® (Microsoft corp, USA). An ANOVA analysis was performed for all osteotomies.

Results:

Figure 3 shows the comparison between signals obtained in the "Bone", "Fracture", and "Hard Bone" states. The ANOVA analysis carried out for all osteotomies showed that the values of τ (respectively of λ) were significantly lower (respectively higher) when the osteotome was in the frontal bone than when it was in the nasal bone ($p < 10^{-10}$ and $p < 10^{-4}$, respectively).

The results of the three classification studies are shown in Fig. 4. Figure 4A, 4B, and 4C show the prediction areas calculated by the SVM model and the values of the parameters for each classification. The boundaries separating the prediction areas calculated by the SVM classifier are displayed as white lines. Figure 4A shows the values of τ and λ when the BOS state after the impact corresponds to "Hard Bone" (blue, dots) and to other states (yellow, crosses). Figure 4B shows the values of $\Delta\tau$ and τ when the BOS state after the impact (before which the BOS state was in the "Bone" state) corresponds to "Fracture" (magenta, crosses) and "Bone" (green, dots). Figure 4C shows the values of $\Delta\tau$ and τ when the BOS state after the impact (before which the BOS state was in the "Fracture" state) corresponds to "Fracture" (pink, crosses) and "Bone" (blue, dots).

The results were implemented by the prediction algorithm in order to predict the state of the BOS after each impact. The results obtained with the algorithm (see Table 1) and with the video motion tracking system were consistent in 83% of the cases. The video motion tracking system found the presence of a fracture which was not predicted by the algorithm in 10% of

cases. Conversely, the video motion tracking system found that the BOS corresponded to "Bone", while a fracture was predicted by the algorithm in 2% of cases. The algorithm failed to predict a BOS corresponding to "HB" in 2% of cases, while a false prediction of "HB" was made in 3% of cases. The third and fourth columns of Table 1 show the results when allowing an error for one and two impacts between the two modalities, respectively.

Discussion:

This study is original as it proposes the use of an instrumented hammer, to guide the surgeon throughout rhinoplasty osteotomies. The results presented for our human anatomical specimen are in qualitative agreement with our previous animal study[17].

When performing osteotomies, anatomical modifications generate a lack of precision, complicating the use of navigational surgical aid systems based on CT-scan imaging. The instrumented hammer allows to perform non-invasive measurements providing information regarding the bone passed through. Coupling the data recovered with this system to CT scan data or a navigated osteotome[20,21] could increase the accuracy of the surgical procedure. The technique described herein is complementary to navigated osteotomes because it predicts the occurrence of uncontrolled fractures, and the proximity of the osteotome to the frontal bone. By comparing bone density to the data acquired intraoperatively using the instrumented hammer, it may become possible to precisely locate the tip of the osteotome, and apply the neuronavigation principles developed in otorhinolaryngologic surgery, neurosurgery, and in a few cases in rhinoplasty in a totally non-invasive manner, and without any preoperative preparation.

However, this study presents several limitations. First, a single variation of the lateral nasal osteotomy was studied here - the low to high path. As such, the prediction model has relatively limited clinical utility, as the model's hypotheses are not necessarily applicable to

other osteotomy paths (low to low, double-level, etc.). The variability in osteotomy trajectories will certainly influence the modeling, as the thickness of the bone along the frontal process of the maxilla, nasal bone proper, and frontal bone may vary considerably based upon the trajectory. Second, the overlying skin was reflected off the nasal bone, which reduced the soft tissue resistance that may have been present in a typical clinical situation with percutaneous osteotomies. Third, the orientation of the osteotome tip to the bony surface wasn't representative of what happens intra-operatively, particularly if the osteotomies are done through a lateral percutaneous approach versus through an intranasal approach at the piriform rim. Fourth, the osteotome was too large and the cutting-edge interface with the bone was likely to have a broader transmission of force than would be seen with a typical (2 mm) osteotome used to perform lateral osteotomies. Fifth, the influence of soft tissues and skin[12] was not taken into account. Such effects could be added to the model as a variable to make it more robust[22]. A future version of the algorithm should focus on reducing the number of "Bone" false positive.

Our results suggest that employing an instrumented hammer in combination with deep learning techniques may constitute an interesting approach to collect information on the biomechanical properties of the bone located at the osteotome tip during rhinoplasty. The significant difference in density between the frontal and nasal bones allows to determine when the osteotome reaches the end of the osteotomy pathway. In addition, the instrumented hammer makes it possible to assess the early onset of bone fractures. Such information is critical to allow adaptation of the following impacts' strength in order to avoid propagation of an existing fracture more than desired. The instrumented hammer could be, with the input of more comprehensive secondary studies, an easy-to-use decision support system that could provide clinicians with relevant and objective information to optimize surgical procedures. In

addition, it could help manufacturers to develop and monitor the effectiveness of surgical instruments used for osteotomies.

Declaration of Competing Interest: None

Funding: N/A

Ethical Approval: N/A

Acknowledgements:

This project has received funding from the European Research Council (ERC) under the European Union's Horizon 2020 research and innovation program (grant agreement No 682001, project ERC Consolidator Grant 2015 BoneImplant). The authors would like to acknowledge the support of the "Prématuration programme" of the CNRS through the Osteome project.

Authorship confirmation statement:

Romain Bosc, Justine Giunta, Anne-Sophie Poudrel, Lara Nokovitch, Giuseppe Rossi, Leo Lamassoure, Guillaume Haiat and Pr Jean-Paul Meningaud have contributed to the conception of this work, the acquisition, the analysis and the interpretation of data. They have drafted the work and revised it critically. They have given their final approval of the version to be published.

Conflicts of Interest Statement:

Romain Bosc, Justine Giunta, Anne-Sophie Poudrel, Lara Nokovitch, Giuseppe Rossi, Leo Lamassoure, Guillaume Haiat and Pr Jean-Paul Meningaud certify that they have no competing interests, no personal financial interests and no other conflict of interest. Nothing to disclose.

References

1. Heidekrueger PI, Juran S, Ehrl D et al. Global aesthetic surgery statistics: a closer look. J Plast Surg Hand Surg 2017;51:270-274.

2. Saban Y. Rhinoplasty: lessons from "errors" : From anatomy and experience to the concept of sequential primary rhinoplasty. HNO 2018;66:15-25.

3. Layliev J, Gupta V, Kaoutzanis C et al. Incidence and Preoperative Risk Factors for Major Complications in Aesthetic Rhinoplasty: Analysis of 4978 Patients. Aesthet Surg J 2017;37:757-767.

4. Shiffman MA, Di Giuseppe A. Advanced Aesthetic Rhinoplasty: Art, Science, and New Clinical Techniques. (Springer-Verlag Berlin Heidelberg, Berlin, Germany). 2013.

5. Dobratz EJ, Hilger PA. Osteotomies. Clin Past Surg 2010;37:301-311.

6. Daniel RK. Mastering rhinoplasty: a comprehensive atlas of surgical techniques with integrated video clips. (Springer-Verlag Berlin Heidelberg, Berlin, Germany). 2010.

7. Siemionow MZ, Eisenmann-Klein M. Nasal reconstruction and aesthetic rhinoplasty. In: Plastic and Reconstructive Surgery. MZ Siemionow and M Eisenmann-Klein, eds. (Springer London Ltd, London, UK). 2010; p. 775.

8. Uraloglu M, Efe G, Karacal R. Lateral Osteotomy Fixation Technique in Rhinoplasty. J Craniofac Surg 2019;30:e600-e603.

9. Mathieu V, Michel A, Flouzat Lachaniette CH et al. Variation of the impact duration during the in vitro insertion of acetabular cup implants. Med Eng Phys 2013;35:1558-1563.

10. Michel A, Bosc R, Mathieu V et al. Monitoring the press-fit insertion of an acetabular cup by impact measurements: influence of bone abrasion. Proc Inst Mech Eng H 2014;228:1027-1034.

11. Michel A, Bosc R, Vayron R et al. In vitro evaluation of the acetabular cup primary stability by impact analysis. J Biomech Eng 2015;137.

12. Bosc R, Tijou A, Rosi G et al. Influence of soft tissue in the assessment of the primary stability of acetabular cup implants using impact analyses. Clin Biomech (Bristol, Avon) 2017;55:7-13.
13. Albini Lomami H, Damour C, Rosi G et al. Ex vivo estimation of cementless femoral stem stability using an instrumented hammer. Clin Biomech (Bristol, Avon) 2020;76:105006.
14. Michel A, Bosc R, Sailhan F et al. Ex vivo estimation of cementless acetabular cup stability using an impact hammer. Med Eng Phys 2016;38:80-86.
15. Dubory A, Rosi G, Tijou A et al. A cadaveric validation of a method based on impact analysis to monitor the femoral stem insertion. J Mech Behav Biomed Mater 2020;103:103535.
16. Hubert A, Rosi G, Bosc R et al. Using an impact hammer to retrieve the geometrical and mechanical properties of a sample during an osteotomy: an in vitro study. J Biomech 2020;142:071009.
17. Lamassoure L, Giunta J, Rosi G et al. Using an Impact Hammer to Perform Biomechanical Measurements during Osteotomies: Study of an Animal Model. Proc Inst Mech Eng H 2021;23:1-8.
18. Tahamiler R, Yener M. Lateral Osteotomy in Rhinoplasty. In: Advanced Aesthetic Rhinoplasty. MA Shiffman and A Di Giuseppe, eds. (Springer, Berlin, Germany). 2013.
19. McHanwell S, Brenner E, Chirculescu ARM et al. The legal and ethical framework governing Body Donation in Europe - A review of current practice and recommendations for good practice. Eur J Anat 2008;12:1-24.
20. Wick EH, Whipple ME, Hohman MH et al. Computer-Aided Rhinoplasty Using a Novel "navigated" Nasal Osteotomy Technique: A Pilot Study. Ann Otol Rhinol Laryngol 2021:3489421996846.

21. Ogino A, Onishi K, Nakamichi M et al. Navigation-Assisted Nasal Bone Osteotomy for Malunited Fracture. J Craniofac Surg 2018;29:156-158.

22. Cortes C, Vapnik V. Support-vector networks. Machine Learning 1995;20:273-297.

Figure:

Figure 1. Experimental configuration considered for the osteotomies.

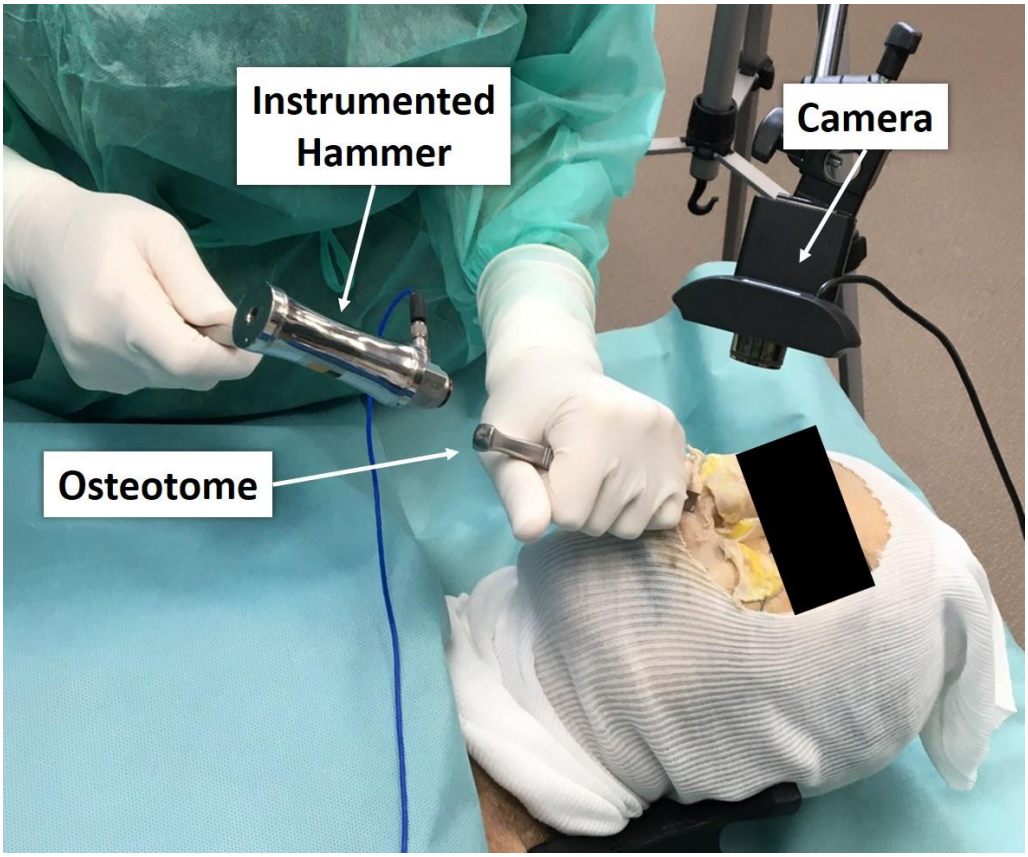

Figure 2. Schematic illustration of the different groups of impacts. The osteotome, bone tissue, and fractures are represented in grey, yellow, and brown, respectively. The corresponding group is indicated for each configuration: I: Bone to Bone (B2B), II: Bone to Fracture (B2F), III: Fracture to Bone (F2B), IV: Fracture to Fracture (F2B).

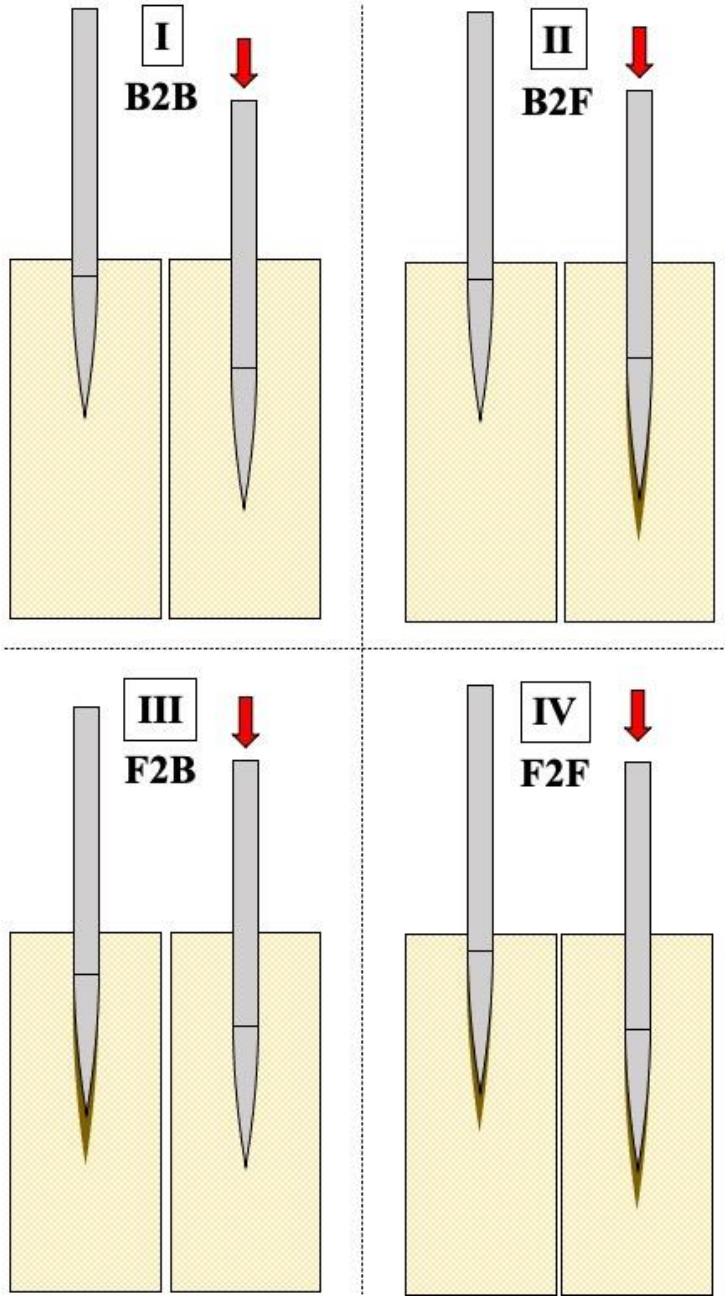

Figure 3. Three examples of signals obtained for each of the different states: “Bone”, “Fracture”, and “Hard Bone”. The corresponding values of τ and λ are indicated.

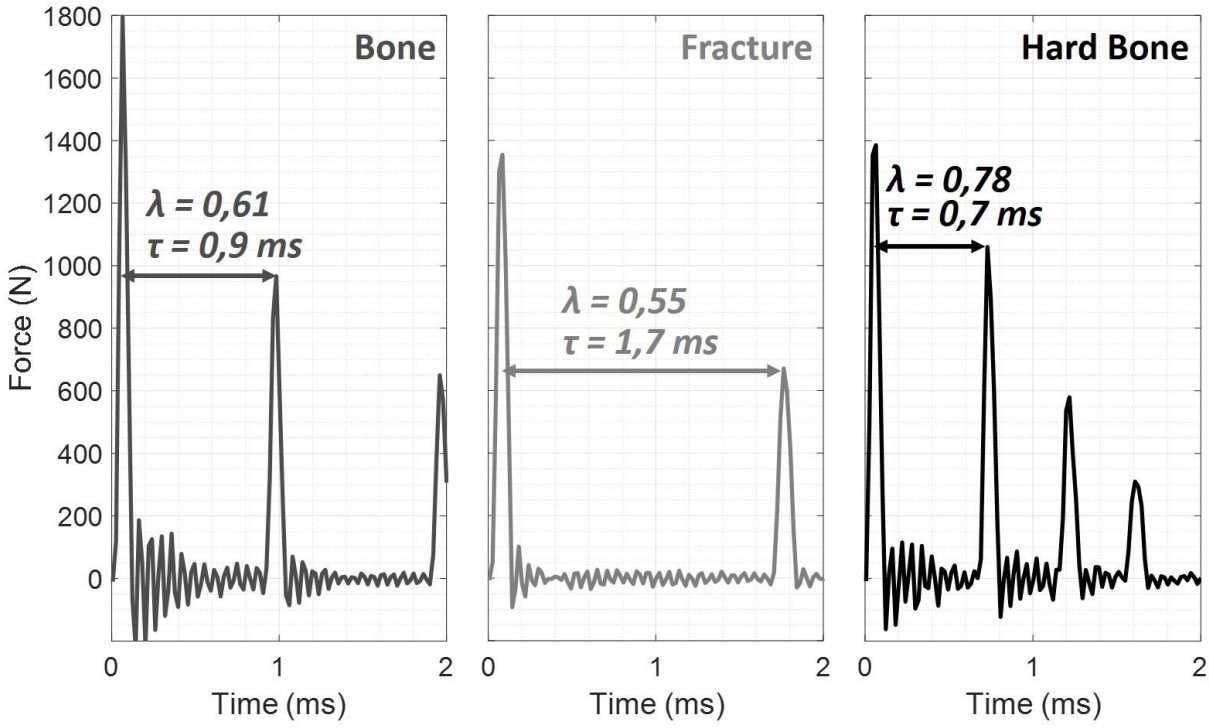

Figure 4. Results of the three classification studies. A: The prediction areas for the "Hard Bone" BOS state and to other BOS states are displayed in dark blue and yellow, respectively. The points belonging to the "Hard Bone" BOS state and to other BOS states are displayed with dots and crosses, respectively. B: The prediction areas for the B2B and B2F groups are displayed in green and magenta, respectively. The points belonging to the B2B and B2F groups are displayed with dots and crosses, respectively. C: The prediction areas for the F2B and F2F groups are displayed in cyan and pink, respectively. The points belonging to the F2B and F2F groups are displayed with dots and crosses, respectively.

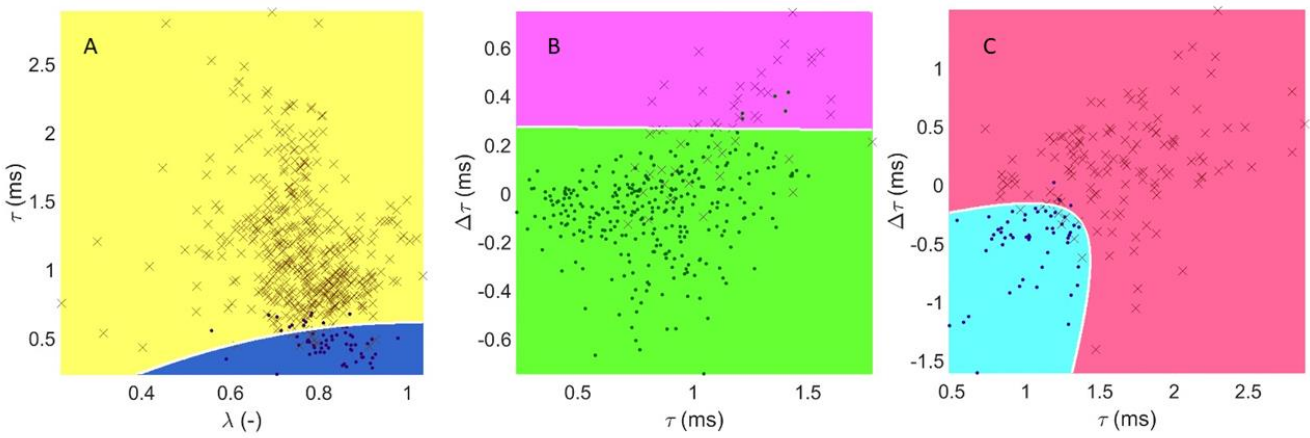

Tables

Table 1. Performance of the algorithm for the prediction of the state of the bone-osteotome system after each impact. The second column shows the raw performances of the algorithm, while the third and fourth column show the performances when allowing a tolerance of 1 and 2 impacts, respectively.

	Correct Predictions	***Fracture* False Positive**	***Bone* False Positive**	***HB* False Positive**
Actual Performance	442/531 (83%)	10/531 (2%)	64/531 (12%)	15/531 (3%)
Perf. with ±1 Tolerance	480/531 (91%)	1/531 (0%)	39/531 (7%)	11/531 (2%)
Perf. with ±2 Tolerance	496/531 (93%)	0/531 (0%)	25/531 (5%)	10/531 (2%)